

Hybridization between the conduction band and 3d orbitals in the oxide-based diluted magnetic semiconductor $\text{In}_{2-x}\text{V}_x\text{O}_3$

M. Kobayashi,¹ Y. Ishida,^{1,*} J. I. Hwang,¹ G. S. Song,¹ M. Takizawa,¹ A. Fujimori,¹ Y. Takeda,² T. Ohkuchi,² T. Okane,² Y. Saitoh,² H. Yamagami,^{2,3} Amita Gupta,⁴ H. T. Cao,⁴ and K. V. Rao⁴

¹*Department of Physics, University of Tokyo, 7-3-1 Hongo, Bunkyo-ku, Tokyo 113-0033, Japan*

²*Synchrotron Radiation Research Unit, Japan Atomic Energy Agency, Sayo-gun, Hyogo 679-5148, Japan*

³*Department of Physics, Faculty of Science, Kyoto Sangyo University, Kyoto 603-8555, Japan*

⁴*Department of Materials Science-Tmfy-MSE, Royal Institute of Technology, Stockholm SE 10044, Sweden*
(Dated: February 4, 2008)

The electronic structure of $\text{In}_{2-x}\text{V}_x\text{O}_3$ ($x = 0.08$) has been investigated using photoemission spectroscopy (PES) and x-ray absorption spectroscopy (XAS). The V 2p core-level PES and XAS spectra revealed trivalent electronic state of the V ion, consistent with the substitution of the V ion for the In site. The V 3d partial density of states obtained by the resonant PES technique showed a sharp peak above the O 2p band. While the O 1s XAS spectrum of $\text{In}_{2-x}\text{V}_x\text{O}_3$ was similar to that of In_2O_3 , there were differences in the In 3p and 3d XAS spectra between V-doped and pure In_2O_3 . The observations give clear evidence for hybridization between the In conduction band and the V 3d orbitals in $\text{In}_{2-x}\text{V}_x\text{O}_3$.

PACS numbers: 75.50.Pp, 75.30.Hx, 78.70.Dm, 79.60.-i

Diluted magnetic semiconductors (DMS's) have been studied intensively since the discovery of ferromagnetism in the III-V DMS $\text{Ga}_{1-x}\text{Mn}_x\text{As}$ [1, 2] because the ferromagnetic interaction between the Mn ions mediated by hole carriers enables us to manipulate both the charge and spin degrees of freedom of electrons [3]. Ferromagnetic DMS's having Curie temperature (T_C) above room temperature have been strongly desired for realistic spintronic applications. Ever since the theoretical prediction by Dietl *et al.* [4] that Mn-doped GaN and ZnO with high hole concentrations should show ferromagnetism above room temperature, wide-gap semiconductors have become promising host materials for high- T_C DMS. In fact, there have been many reports on room temperature ferromagnetism in oxide-based DMS's such as Co-doped TiO_2 [5], Co-doped SnO_2 [6], and Mn-doped ZnO [7].

Recently, In_2O_3 -based DMS's have attracted much attention because of the reports of room temperature ferromagnetism in not only light transition-metal (TM) but also heavy TM doped In_2O_3 [8, 9, 10, 11, 12, 13, 14, 15, 16, 17, 18, 19, 20] and of the potential of the host material In_2O_3 for applications. Here, In_2O_3 has a band gap of ~ 3.5 eV, is an *n*-type semiconductor, and crystallizes in the cubic bixbyite structure, where In atoms are coordinated by six oxygens forming octahedral (O_h) and orthorhombic (D_{2h}) octahedra and neighboring octahedra are shared with their corners and edges [21, 22], and Sn-doped In_2O_3 (ITO) has been famous for its high electrical conductivity and transparency [23, 24]. Magnetic force microscopy observations of $\text{In}_{2-x}\text{Cr}_x\text{O}_{3-\delta}$ and $\text{In}_{2-x}\text{Ni}_x\text{O}_3$ have demonstrated that the topological undulations correspond to the strength of magnetic re-

sponse, indicating a uniform distribution of magnetic domains in these materials [12, 18]. Reports of In_2O_3 -based DMS's have suggested relationship between the electrical conductivity and ferromagnetism through measurements of, e.g., anomalous Hall effects [16, 17, 18, 19, 20]. As In_2O_3 -based DMS's are candidates for room-temperature ferromagnetic DMS's, the knowledge of their electronic structure is necessary to understand of the origin of the ferromagnetism.

Photoemission spectroscopy (PES) and x-ray absorption spectroscopy (XAS) are powerful tools to investigate electronic structure of materials. XAS, which means photon absorption from a core-level electron into unoccupied states, is an element specific technique to study the electronic structure. $2p \rightarrow 3d$ resonant photoemission spectroscopy (RPES) enables us to extract the 3d partial density of states (PDOS) in the valence band. In this work, we have performed PES and XAS measurements on $\text{In}_{2-x}\text{V}_x\text{O}_3$ (IVO) thin films in order to obtain a fundamental understanding of the electronic structures. The valence state of the doped V ion has been determined by core-level x-ray photoemission spectroscopy (XPS) and XAS. Effects of doping on the electronic structure of the host material have been approached by V $2p \rightarrow 3d$ RPES and XAS at the O and In edges.

Each of In_2O_3 and $\text{In}_{2-x}\text{V}_x\text{O}_3$ ($x = 0.08$) thin films was highly oriented normal to the plane of a sapphire(0001) substrate by the pulsed laser deposition technique. During the deposition, the substrate temperature was kept at ~ 400 °C. The total thickness of the deposited layer was ~ 500 nm. X-ray diffraction confirmed that the thin film had the cubic bixbyite structure and no secondary phase was observed. Details of the sample fabrication are given in Ref. [14]. The V concentration x in the thin films was estimated from the intensity of the V 2p core-level PES spectrum. Ferromagnetism above room temperature was confirmed by magnetization mea-

*Present address: RIKEN, SPring-8 Center, Sayo-cho, Hyogo 679-5148, Japan

measurements using a SQUID magnetometer (Quantum Design, Co. Ltd.).

RPES and XAS measurements were performed at the soft x-ray beam line BL23SU of SPring-8 [25, 26]. The monochromator resolution was $E/\Delta E > 10,000$. XAS signals were measured by the total electron yield method. The background of the XAS spectra was assumed to be a hyperbolic tangent function. The RPES and XPS measurements were performed in a vacuum below 1.0×10^{-7} Pa using Gammadata Scienta SES-2000 and SES-100 hemispherical analyzers, respectively. A Mg- $K\alpha$ x-ray source ($h\nu = 1253.6$ eV) was employed for the XPS measurements. In the PES measurements, photoelectrons were collected in the angle integrated mode at room temperature. The total resolution of the RPES and XPS measurements including temperature broadening were ~ 300 and ~ 800 meV, respectively. Sample surface was cleaned by cycles of Ar^+ -ion sputtering. Cleanliness of the sample surface was checked by the absence of a high binding-energy shoulder in the O $1s$ spectrum and C $1s$ contamination by XPS. The position of the Fermi level (E_F) was determined by measuring PES spectra of evaporated gold which was electrically in contact with the samples.

First, we discuss about the valence state of the V ions in IVO. Figure 1 shows the V $2p$ core-level spectra of IVO and various vanadium oxides. The binding energy (E_B) of a core-level peak position is related to its charge state and, in general, becomes larger with increasing valency. In fact, it has been reported that the E_B of the V $2p_{3/2}$ peak increases with valency of V as shown in Fig. 1(a) [27]. By comparing the peak position of the V $2p_{3/2}$ core level of IVO with those of the other vanadium oxides, the valence state of V in In_2O_3 is found to be trivalent V^{3+} (d^2). Figure 1(b) shows the V $2p$ XAS spectra of IVO

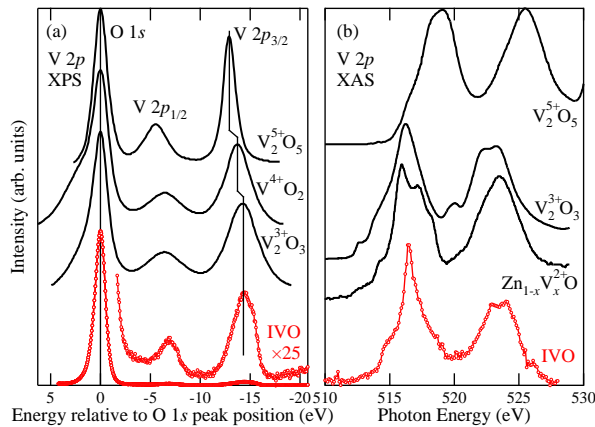


FIG. 1: V $2p$ core-level spectra of $\text{In}_{2-x}\text{V}_x\text{O}_3$ (IVO) with $x = 0.08$. (a) V $2p$ XPS spectra compared with those of other vanadium oxides [27]. (b) V $2p$ XAS spectra compared with those of other vanadium oxides $\text{Zn}_{1-x}\text{V}_x\text{O}$ [29], V_2O_3 [28], and V_2O_5 [30].

and several vanadium oxides. The line shape of the V $2p$ spectrum of IVO is similar to that of V_2O_3 (V^{3+}) [28] rather than that of $\text{Zn}_{1-x}\text{V}_x\text{O}$ (V^{2+}) [29] and of V_2O_5 (V^{5+}) [30], consistent with the observation of the V $2p$ XPS. The results suggest that the electronic structure of the doped V ion in IVO is close to that of the V ion in V_2O_3 , i.e., V is in the trivalent V^{3+} state octahedrally coordinated by oxygens. Therefore, it is likely that the doped V ions are substituted for the In sites.

In order to obtain an understanding of the electronic structure of the V ion in the valence band, we measured V $2p \rightarrow 3d$ resonant photoemission spectra of IVO. Figure 2(b) shows the valence-band PES spectra of IVO taken at various photon energies in the V $2p \rightarrow 3d$ core-excitation region. Energy difference between the top of the O $2p$ bands and E_F is ~ 3.0 eV, comparable to the band gap of $\text{In}_2\text{O}_3 \sim 3.5$ eV, indicating that in the IVO sample E_F is located near the bottom of the conduction band. We observed clear resonant enhancement in the valence band. The PES intensity as a function of photon energy ($h\nu$), i.e., constant-initial-state (CIS) spectrum, at $E_B = 1.7$ eV demonstrates that the enhancement is proportional to the intensity of the V $2p$ XAS as shown in Fig. 2(a). The on- and off-resonance spectra were chosen as measured at $h\nu = 516.5$ eV and 513 eV, respectively. The difference between the on- and off-resonance spectra yields the V $3d$ PDOS. Although the relative intensities of different spectral features change with photon energy due to the effects of transition matrix elements and of the resonance, the structures (peak positions) of the V

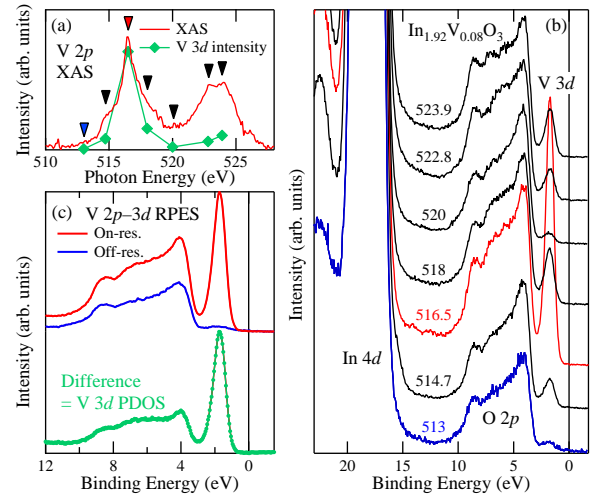


FIG. 2: V $2p \rightarrow 3d$ resonant photoemission spectra in the valence band of $\text{In}_{2-x}\text{V}_x\text{O}_3$ ($x = 0.08$). (a) V $2p$ XAS spectrum and the intensity of the V $3d$ peak at $E_B = 1.7$ eV as functions of photon energy. (b) A series of spectra measured at $h\nu$'s denoted by triangles in (a). (c) Top: On- ($h\nu = 516.5$ eV) and off-resonance ($h\nu = 513$ eV) spectra. Bottom: On- and off-resonance difference spectrum representing the V $3d$ partial density of states (PDOS).

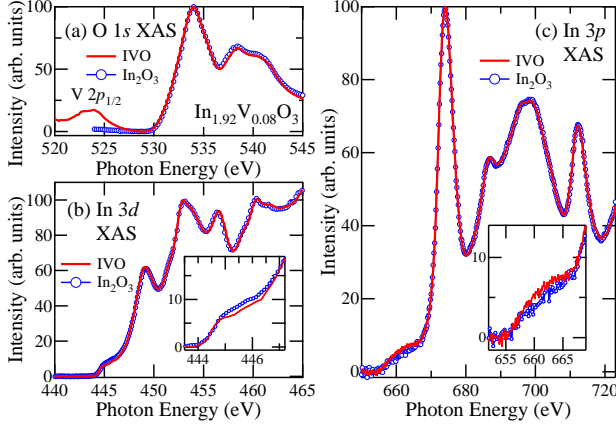


FIG. 3: X-ray absorption spectra of $\text{In}_{2-x}\text{V}_x\text{O}_3$ (IVO) with $x = 0.08$ measured at In and O absorption edges related to the host In_2O_3 . (a) O K XAS spectra. (b), (c) In $3d$ and $3p$ XAS spectra, respectively. The insets show enlarged plots in the pre-edge region.

$3d$ PDOS are independent of photon energy, implying that the V ions are in a single electronic state. The V $3d$ PDOS shows a peak above the O $2p$ band, that is, in the middle of the band gap of In_2O_3 , as shown in Fig. 2(c). The narrow width and strong intensity of the peak imply the localized nature of the V $3d$ orbitals in the valence band, i.e., weak V $3d$ – O $2p$ mixing in IVO.

In n -type DMS's, electronic states near the bottom of the conduction band are expected to be important for carrier-induced ferromagnetism since E_F is located there. Because the valence band of the host semiconductor is usually occupied, XAS spectra measured at the absorption edges of the host semiconductor reflect the unoccupied electronic states, namely, the conduction band, and are useful for the investigation of the electronic structure of n -type DMS's. Figure 3 shows XAS spectra measured at absorption edges of In and O, and compares them between V-doped and pure In_2O_3 . The O $1s$ XAS spectrum of IVO is nearly identical to that of In_2O_3 as shown in Fig. 3(a). It has been reported that the O $1s$ XAS spectrum of Fe-doped In_2O_3 differs from that of pure In_2O_3 , and that the difference is induced by hybridization of the Fe $3d$ orbitals with the O $2p$ band [15]. The observation implies weaker hybridization between the O $2p$ band and the V $3d$ orbitals in IVO than that between O $2p$ and Fe $3d$ in $\text{In}_{2-x}\text{Fe}_x\text{O}_3$, consistent with the result of the V $2p \rightarrow 3d$ RPES. In contrast, the In $3p$ and $3d$ XAS spectra were changed by V doping, i.e., there are difference between the XAS spectra of IVO and these of pure In_2O_3 in both pre-edge regions as shown in Figs. 3(b) and 3(c). The observations clearly indicate hybridization between the In $5sp$ conduction band and the V $3d$ orbitals in IVO.

Based on the above findings, we shall discuss about the electronic structure of In_2O_3 -based DMS's, in particular, those doped with light-TM atoms. Electronic structure

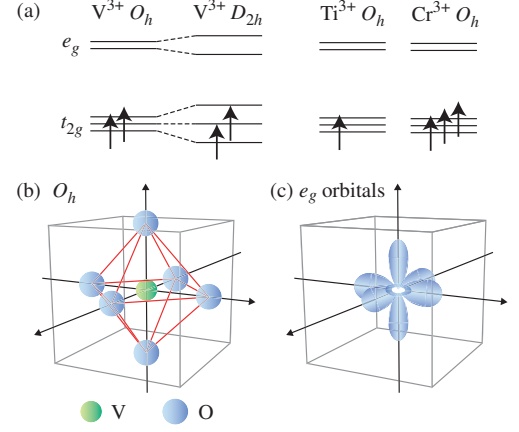


FIG. 4: $3d$ electronic structure of the V ion of $\text{In}_{2-x}\text{V}_x\text{O}_3$. (a) A schematic representation of the electronic structure in the V ion. Those of the Ti^{3+} and Cr^{3+} ion in a O_h crystal field are also presented. (b) Octahedral coordination of the O atoms. (c) e_g orbitals.

of a TM atom octahedrally coordinated by oxygens splits into two-fold degenerate e_g and three-fold degenerate t_{2g} levels due to ligand crystal fields. In IVO, the V^{3+} ($3d^2$) ion substituting for the In site has two electrons in the t_{2g} levels (or the two lowest levels splitted from the t_{2g} level due to the D_{2h} symmetry) as shown in Fig. 4(a). Because the e_g orbitals are directed toward the O atoms as shown in Figs. 4(b) and 4(c), the O $2p$ band can hybridize with the e_g orbitals stronger than the t_{2g} orbitals. Indeed, the Slater-Koster parameter ($pd\sigma$), which represents transfer integrals between the $3d$ e_g and ligand p orbitals, has an absolute value about twice larger than ($pd\pi$), which represents transfer integrals between the $3d$ t_{2g} and ligand p orbitals [31]. Considering the result of O $1s$ XAS, hybridization between the O $2p$ band and the e_g orbitals is expected to be weak. It is probable that the t_{2g} orbitals hybridize dominantly with the In band. Light TM ions Ti^{3+} and Cr^{3+} under the O_h crystal field only have electron(s) in the t_{2g} levels, too [Fig. 4(a)]. It follows from those arguments that for light TM-doped In_2O_3 , hybridization between the host conduction band and the $3d$ t_{2g} orbitals should be taken into consideration to understand their electronic properties.

Considering the present observations, we shall discuss about the mechanism of the ferromagnetism in $\text{In}_{2-x}\text{V}_x\text{O}_3$. The bottom of the conduction band of In_2O_3 are mainly composed of the In $5s$ bands [21]. For n -type DMS's, the electronic structure near the bottom of the conduction band is important, i.e., s - d exchange interaction may play an essential role rather than the p - d exchange interaction. It is possible that hybridization between the In $5s$ and V $3d$ orbitals as observed in $3p$ XAS strengthens the s - d exchange interaction, as in the case of the host conduction band – Co $3d$ orbital exchange interaction in $\text{Ti}_{1-x}\text{Co}_x\text{O}_2$ [32]. Generally speaking, be-

cause in wide-gap semiconductors the effective mass m^* is large, the magnetic splitting due to the exchange term in Hamiltonian ($s,p-d$ exchange interaction) is greater than the spin splitting of the host valence and conduction bands predicted by ordinary sp band theory, and the exchange contribution can be expressed as a large effective g factor, which is given by

$$g_{\text{eff}} = g^* + \Delta g_{\text{ex}},$$

$$\Delta g_{\text{ex}} = \alpha M / (g_{\text{TM}} \mu_{\text{B}}^2 H),$$

where g^* is the band g factor, g_{TM} is the g factor of the $3d$ ions, α is the exchange constant, and μ_{B} is the Bohr magneton, that is, $|\Delta g_{\text{ex}}| \gg |g^*|$ for wide-gap semiconductors [33]. Therefore, the $s-d$ exchange interaction accompanied by the spin splitting of the conduction band is expected to be dominant in $\text{In}_{2-x}\text{V}_x\text{O}_3$. In such a case, magnetic circular dichroism signal at the optical absorption edge should be measurable. Additional measurements which are related to the spin splitting of the conduction band are highly desirable. Since the extent of $3d$ orbitals diminish with increasing number of $3d$ electrons, effects of cation- $3d$ hybridization may weaken in heavy TM-doped DMS's.

Assuming that light TM-doped In_2O_3 DMS's have common properties, we can discuss about the role of oxygen vacancies in In_2O_3 -based DMS's. The oxygen vacancy is a major defect in oxides and acts as a double donor. In addition to electron doping by the vacancies, it has recently been proposed that the existence of oxygen vacancies themselves affects the ferromagnetic properties of oxide-based DMS's through the formation of the donor-impurity band (in this case, the oxygen vacancies are the centers of bound magnetic polarons) [34], and reported that, even in non-magnetic oxide, the ferromagnetism can be induced by the oxygen vacancies [35, 36]. For light TM-doped In_2O_3 DMS's, there are several works related to oxygen vacancies. Philip *et al.* [18] have reported that while $\text{Cr}:\text{In}_2\text{O}_3$ thin films deposited at high oxygen pressure (20 mTorr) show paramagnetic behavior, films deposited at low oxygen pressure (0.35 mTorr) exhibits ferromagnetic properties, where the low pressure growth induces in the thin films with electron carriers through the oxygen vacancies. Kharel *et al.* [37] have found that while air annealed Cr-doped In_2O_3 film and bulk samples do not show ferromagnetism, samples

annealed in a high vacuum are ferromagnetic due to the creation of oxygen vacancies. A first-principle electronic-structure calculation of In_2O_3 has predicted that when electrons are localized around the oxygen vacancy, the In-In bond is reinforced remarkably while the In-O bond is significantly weakened [21]. Considering this result together with the experimental findings, it is possible that, besides the electron carrier doping, the presence of oxygen vacancy augments the exchange interaction between the In conduction band and the $3d$ orbitals. This effect may be stronger for light TM-doped In_2O_3 DMS's than heavy TM-doped ones because of the shrinkage of the $3d$ orbitals with the number of $3d$ electrons. In order to set whether this consideration is valid or not, systematic measurements of In_2O_3 -based DMS's with independently controlled oxygen vacancies and carrier concentrations are desirable.

In conclusion, we have performed PES and XAS studies of $\text{In}_{2-x}\text{V}_x\text{O}_3$ thin films in order to investigate their electronic structure and its relationship with ferromagnetism. From comparison with previous reports, the V $3d$ ions are expected to be trivalent states, indicating that the V ion substitutes for the In site. The V $3d$ PDOS in valence band has been observed using RPES technique and shows a sharp peak within the band gap of In_2O_3 , implying the localized nature of the V $3d$ orbitals in the valence band. There are differences of XAS spectra measured at In $3p$ and $3d$ edges although the O K XAS spectrum is independent of V doping. Based on the findings, it is likely that the $s-d$ exchange interaction is dominant for the ferromagnetism in $\text{In}_{2-x}\text{V}_x\text{O}_3$. For light TM-doped In_2O_3 , the role of oxygen vacancy has been discussed. The present results point to a need for taking into account hybridization between the host conduction band and $3d$ orbitals in In_2O_3 -based DMS's, especially for light TM doped ones. We believe that the findings will promote further systematic studies of n -type oxide-based DMS's.

This work was supported by a Grant-in-Aid for Scientific Research in Priority Area "Spin Current: Its Creation and Control" (19048012) from MEXT, Japan. Work in Sweden is supported by the Swedish Agency VINNOVA, and the Carl Tryggers Stiftelse. MK and MT acknowledge support from the Japan Society for the Promotion of Science for Young Scientists.

-
- [1] H. Ohno, A. Shen, F. Matsukura, A. Oiwa, A. Endo, S. Katsumoto, and Y. Iye, Appl. Phys. Lett. **69**, 363 (1996).
 - [2] F. Matsukura, H. Ohno, A. Shen, and Y. Sugawara, Phys. Rev. B **57**, R2037 (1998).
 - [3] H. Ohno, Science **281**, 951 (1998).
 - [4] T. Dietl, H. Ohno, F. Matsukura, J. Cibert, and D. Fermand, Science **287**, 1019 (2000).
 - [5] Y. Matsumoto, M. Murakami, T. Shono, T. Hasegawa, T. Fukumura, M. Kawasaki, P. Ahmet, T. Chikyow, S.-Y. Koshihara, and H. Koinuma, Science **291**, 854 (2001).
 - [6] S. B. Ogale, R. J. Choudhary, J. P. Buban, S. E. Lofland, S. R. Shinde, S. N. Kale, V. N. Kulkarni, J. Higgins, C. Lanci, J. R. Simpson, N. D. Browning, S. Das Sarma, H. D. Drew, R. L. Greene, and T. Venkatesan, Phys. Rev. Lett. **91**, 077205 (2003).
 - [7] P. Sharma, A. Gupta, K. V. Rao, F. J. Owens, R. Sharma, R. Ahuja, J. M. O. Guillen, B. Johansson, and G. A. Gehring, Nat. Mater. **2**, 673 (2003).

- [8] J. Philip, N. Theodoropoulou, G. Berera, J. S. Moodera, and B. Satpati, *Appl. Phys. Lett.* **85**, 777 (2004).
- [9] Y. K. Yoo, Q. Xue, H.-C. Lee, S. Cheng, X.-D. Xiang, G. F. Dionne, S. Xu, J. He, Y. S. Chu, S. D. Preite, S. E. Lofland, and I. Takeuchi, *Appl. Phys. Lett.* **86**, 042506 (2005).
- [10] N. H. Hong, J. Sakai, N. T. Huong, and V. Brizé, *Appl. Phys. Lett.* **87**, 102505 (2005).
- [11] G. Peleckis, X. L. Wang, and S. X. Dou, *Appl. Phys. Lett.* **88**, 132507 (2006).
- [12] N. H. Hong, J. Sakai, N. T. Huong, A. Ruyter, and V. Brizé, *J. Phys.: Condens. Mat.* **18**, 6897 (2006).
- [13] G. Peleckis, X. Wang, and S. X. Dou, *Appl. Phys. Lett.* **89**, 022501 (2006).
- [14] A. Gupta, H. T. Cao, K. Parekh, K. V. Rao, A. R. Raju, and U. V. Waghmare, *J. Appl. Phys.* **101**, 09N513 (2007).
- [15] O. D. Jayakumar, I. K. Gopalakrishnan, S. K. Kulshreshtha, A. Gupta, K. V. Rao, D. V. Louzguine-Luzgin, A. Inoue, P.-A. Glans, J.-H. Guo, K. Samanta, M. K. Singh, and R. S. Katiyar, *Appl. Phys. Lett.* **91**, 052504 (2007).
- [16] J. He, S. Xu, Y. K. Yoo, Q. Xue, H.-C. Lee, S. Cheng, X.-D. Xiang, G. F. Dionne, and I. Takeuchi, *Appl. Phys. Lett.* **86**, 052503 (2005).
- [17] H. S. Kim, S. H. Ji, H. Kim, S.-K. Hong, D. Kim, Y. E. Ihm, and W. K. Choo, *Solid State Commun.* **137**, 41 (2006).
- [18] J. Philip, A. Punnoose, B. I. Kim, K. M. Reddy, S. Layne, J. O. Holmes, B. Satpati, P. R. Leclair, T. S. Santos, and J. S. Moodera, *Nat. Mater.* **5**, 298 (2006).
- [19] Z. G. Yu, J. He, S. Xu, Q. Xue, O. M. J. van't Erve, B. T. Jonker, M. A. Marcus, Y. K. Yoo, S. Cheng, and X.-D. Xiang, *Phys. Rev. B* **74**, 165321 (2006).
- [20] J. Stankiewicz, F. Villuendas, and J. Bartolomé, *Phys. Rev. B* **75**, 235308 (2007).
- [21] I. Tanaka, M. Mizuno, and H. Adachi, *Phys. Rev. B* **56**, 3536 (1997).
- [22] L. Marsella and V. Fiorentini, *Phys. Rev. B* **69**, 172103 (2004).
- [23] H. Kim, C. M. Gilmore, A. Piqué, J. S. Horwitz, H. Mat-toussi, H. Murata, Z. H. Kafafi, and D. B. Chrisey, *J. Appl. Phys.* **86**, 6451 (1999).
- [24] C. G. Granqvist and A. Hultåker, *Thin Solid Films* **411**, 1 (2002).
- [25] J. Okamoto, K. Mamiya, S.-I. Fujimori, T. Okane, Y. Saitoh, Y. Muramatsu, A. Fujimori, S. Ishikawa, and M. Takano, *AIP Conf. Proc.* **705**, 1110 (2004).
- [26] Y. Saitoh, T. Nakatani, T. Matsushita, A. Agui, A. Yoshigoe, Y. Teraoka, and A. Yokoya, *Nucl. Instrum. Methods Phys. Res. Sect. A* **474**, 253 (2001).
- [27] G. A. Sawatzky and D. Post, *Phys. Rev. B* **20**, 1546 (1979).
- [28] J. Park, Thesis (University of Michigan, 1993).
- [29] Y. Ishida, J. I. Hwang, M. Kobayashi, Y. Takeda, K. Mamiya, J. Okamoto, S.-I. Fujimori, T. Okane, K. Terai, Y. Saitoh, Y. Muramatsu, A. Fujimori, A. Tanaka, H. Saeki, T. Kawai, and H. Tabata, *Appl. Phys. Lett.* **90**, 022510 (2007).
- [30] A. Gloskovskii, S. A. Nepijko, G. Schönhense, H. A. Therese, A. Reiber, H. C. Kandpal, G. H. Fecher, C. Felser, W. Tremel, and M. Klimenkov, *J. Appl. Phys.* **101**, 084301 (2007).
- [31] W. A. Harrison, *Electronic Structure and the Properties of Solids* (Dover, New York, 1989).
- [32] J. W. Quilty, A. Shibata, J.-Y. Son, K. Takubo, T. Mizokawa, H. Toyosaki, T. Fukumura, and M. Kawasaki, *Phys. Rev. Lett.* **96**, 027202 (2006).
- [33] J. K. Furdyna, *J. Appl. Phys.* **64**, R29 (1988).
- [34] J. M. D. Coey, M. Venkatesan, and C. B. Fitzgerald, *Nat. Mater.* **4**, 173 (2005).
- [35] A. Sundaresan, R. Bhargavi, N. Rangarajan, U. Siddesh, and C. N. R. Rao, *Phys. Rev. B* **74**, 161306(R) (2006).
- [36] N. H. Hong, J. Sakai, and F. Gervais, *J. Magn. Magn. Mater.* **316**, 214 (2007).
- [37] P. Kharel, C. Sudakar, M. B. Sahana, G. Lawes, R. Suryanarayanan, R. Naik, and V. M. Naik, *J. Appl. Phys.* **101**, 09H117 (2007).